Nonlinear evolution of the plasma beat wave: Compressing the laser beat notes via electromagnetic cascading

Serguei Kalmykov* and Gennady Shvets
Department of Physics and Institute for Fusion Studies, The University of Texas at Austin, One University Station C1500, Austin, Texas 78712, USA
(Received 22 November 2005; published 18 April 2006)

The near-resonant beat wave excitation of an electron plasma wave (EPW) can be employed for generating the trains of few-femtosecond electromagnetic (EM) pulses in rarefied plasmas. The EPW produces a comoving index grating that induces a laser phase modulation at the difference frequency. As a result, the cascade of sidebands red and blue shifted by integer multiples of the beat frequency is generated in the laser spectrum. The bandwidth of the phase-modulated laser is proportional to the product of the plasma length, laser wavelength, and amplitude of the electron density perturbation. When the beat frequency is lower than the electron plasma frequency, the redshifted spectral components are advanced in time with respect to the blueshifted ones near the center of each laser beat note. The group velocity dispersion of plasma compresses so chirped beat notes to a few-laser-cycle duration thus creating a train of sharp EM spikes with the beat periodicity. Depending on the plasma and laser parameters, chirping and compression can be implemented either concurrently in the same, or sequentially in different plasmas. Evolution of the laser beat wave and electron density perturbations is described in time and one spatial dimension in a weakly relativistic approximation. Using the compression effect, we demonstrate that the relativistic bistability regime of the EPW excitation [G. Shvets, Phys. Rev. Lett. **93**, 195004 (2004)] can be achieved with the initially subthreshold beat wave pulse.

DOI: 10.1103/PhysRevE.73.046403 PACS number(s): 52.35.−g, 52.38.−r

I. INTRODUCTION

An electron plasma wave (EPW) is a natural tool for manipulating the properties of intense radiation beams. It can be used for up shifting the laser frequency [1], for enhancing the self-focusing of copropagating [2,3] and counter-propagating [4] radiation beams, for the resonant self-modulation of the laser amplitude [5], and for coupling the signal and pump lasers in the parametric amplifier [6]. Also, the high-amplitude EPW driven by a short laser pulse can induce the pulse shrinkage with time [7].

In this paper we show that the near-resonant excitation of the EPW strongly modifies an originally two-color driving laser beam: a train of few-cycle relativistically intense spikes can be created from the initially nonrelativistic amplitude-modulated pulse. It is known for a long time that the ponderomotive force (beat wave) of the two-color laser [8–12] can provide a controlled excitation of the EPW. When the beat wave frequency Ω is close to the electron Langmiur frequency $\omega_p=\sqrt{4\pi e^2 n_0/m_e}$ (n_0 is an electron plasma density, m_e and $-|e|$ are the electron rest mass and charge), the near-resonantly driven EPW can reach a high amplitude and become nonlinear. In this case, the laser and EPW dynamics becomes very multifaceted. The nonlinear plasma wave is highly sensitive to the variations of frequency and amplitude of the ponderomotive force. For example, by chirping the beat frequency [13] the EPW excitation can be enhanced by the autoresonance effect. Downshifting the beat frequency from the plasma resonance ($\Omega<\omega_p$) can also result in the large-amplitude wake excitation due to the effect of relativistic bistability [14,15]. Conversely, the driven electron density perturbations can cause the laser amplitude modulation, either transverse [2,3] or longitudinal [16]. Therefore, the performance of the beat wave scheme critically depends on the self-consistent evolution of the light and plasma waves that includes effects of numerous plasma nonlinearities [17]. The nonlinear processes of relativistic self-phase modulation [18], stimulated forward Raman scattering [19,20] (SFRS), and electromagnetic cascading [2,3,16,21,22] (EMC) broaden the laser frequency bandwidth. At the same time, the group velocity dispersion (GVD) of radiation results in the amplitude modulation of the frequency broadened laser. In this paper we incorporate the physically important aspects of the beat wave evolution in a homogeneous fully ionized plasma (nonlinear frequency shifts of the waves, nonlinear excitation, and relativistic bistability of the EPW, electromagnetic cascading, amplitude and phase modulation of the laser, and SFRS) in a consistently derived one-dimensional (1D) weakly nonlinear nonstationary model. In this sense, our work finalizes the weakly nonlinear 1D plasma beat wave theory.

We apply the developed model to the particular effect of compressing the laser beat notes to a few-cycle duration (whereby generating trains of few-femtosecond radiation spikes of relativistic intensity; the spikes are separated in time by the beat period $\tau_b=2\pi/\Omega$) [16]. The beat note compression requires the frequency downshifted ($\Omega<\omega_p$) beat wave pulse of initially moderate amplitude. In this case, the broad bandwidth necessary for compression is generated mainly due to the EMC effect. At every point of the perturbed plasma, the EPW creates an index grating comoving with the laser beams. Hence, the laser frequency becomes modulated at a difference frequency Ω, which results in a

*Electronic address: kalmykov@physics.utexas.edu

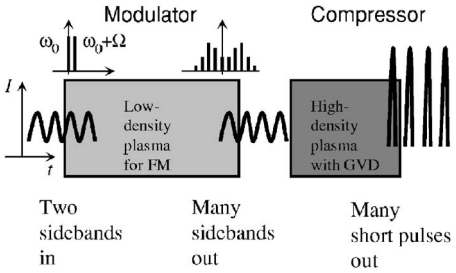

FIG. 1. Schematic of the two-stage cascade compressor. The frequency modulation (FM) occurs in a rarefied plasma. Denser plasma is used for the compression of beat notes.

cascade of Stokes and anti-Stokes sidebands shifted by integer multiples of Ω from the laser fundamental ω_0. The effect of EMC has been known in physics of laser-plasma interactions since early 1970s when Cohen *et al.* [21] suggested to enhance plasma heating by the decay of the cascade-driven EPW. Later on, the EMC was considered as a plasma wave diagnostic in the plasma beat wave accelerator [22]. Systematic study [2,3] of plasma waveguiding options provided by the nonlinear interaction of laser beams with the cascade-driven EPW revealed an enhanced self-focusing of the co-propagating beams detuned in frequency below plasma resonance ($\Omega < \omega_p$). Calculations of Refs. [2,3] describe the nonstationary cascade evolution in two dimensions (2D) in the planar and three dimensions (3D) in cylindrical geometry, take a full account of the relativistic nonlinearities of both cascade components and the EPW. Neither of the preceding papers payed attention to the longitudinal transport of the cascade energy due to the effect of nonzero GVD and consequent amplitude distortion of the laser. Our work fills this gap by concentrating on the 1D compression of laser beatnotes due to the EMC and GVD.

We prove that the GVD completely dominates the evolution of weakly-relativistic beat wave (with intensity of initial beams over 10^{16} W/cm^2) in either centimeter-scale rarefied ($n_0 \sim 10^{18}$ cm^{-3}) or millimeter-scale dense plasmas ($n_0 \gtrsim 10^{19}$ cm^{-3}). We show that the EPW driven *below* resonance, $\Omega < \omega_p$, chirps the laser frequency in a very special way: near the center of each laser beat note the redshifted sidebands are advanced in time with respect to the blue-shifted ones. The GVD can compress thus chirped beatnotes to a few-laser-cycle duration provided the laser bandwidth tends to ω_0. The effect of GVD is controllable: proper adjustment of the plasma and laser parameters can reduce it while preserving the desirable bandwidth. In this case, the cascade compression can be made in two stages [16] (see Fig. 1): (i) a low-density plasma (the modulator) with $\Omega < \omega_{p(M)}$ is used for the frequency modulation of initially two-frequency laser, and (ii) a higher-density plasma (the compressor) with $\omega_{p(C)} \gg \Omega$ serves for the beat note compression. Therefore, a train of sharp electromagnetic spikes of intensity by several orders of magnitude higher than ionization threshold for any medium can be generated. Similar concept of using Raman cascades for radiation beams compression in molecular gases has been successfully tested in experiments [23] at low laser intensities ($\ll 10^{14}$ W/cm^2). The technique of the EMC compression in gases is not appropriate for applications requiring high laser intensity. One such application is using multiple short laser pulses with a tunable time delay for the coherent generation of plasma waves [24–26]. Making a sequence of several *independent* ultrashort high-intensity laser pulses with the terahertz repetition rate could be a major experimental challenge [24]. The approach discussed in our paper suggests a viable path to creating such pulse trains at weakly relativistic intensity.

The outline of the paper is as follows. In Sec. II we derive the basic theoretical model (Sec. II A) and analyze the basic scalings for the EMC and the cascade compression (Sec. II B). In a realistic plasma, the EMC is a complicated interplay between the sideband coupling through the driven electron density perturbations, GVD of radiation, nonlinearities due to the relativistic increase of an electron mass, and SFRS. Fully nonlinear simulations presented in Sec. III account for all these effects and describe the cascade development in either two-stage (Sec. III A) or single-stage (Sec. III B) compressor. Because the longest time scale of the problem is only a few ion plasma periods, parametric decay of the EPW [27] and consequent plasma heating [21] are insignificant and thus ignored. The simulation parameters of Secs. III A and III B are optimized so as to eliminate the relativistic nonlinearities and SFRS. We also prove that the compression effect persists in the very rough conditions of dense plasmas and short subrelativistic lasers of a possible real-scale experiment [28]. When the parameters of the setup are not optimized, the SFRS can be seeded by the plasma wake driven by the beatwave pulse of finite duration. Contribution from the SFRS into the cascading process is discussed in Sec. III C. Numerical analysis of the SFRS manifestation reveals the conditions which the beat wave pulse should satisfy to eliminate this potentially adverse instability. In Sec. III D we have shown for the first time that, with the help of the cascade compression, the relativistic bistability of the EPW can manifest in the dynamic simulations with the laser initially not optimized to meet the bistabilty threshold [14,15]. Conclusion gives the summary of the results.

II. ONE-DIMENSIONAL THEORY OF EMC

A. Basic equations

We assume that the laser duration does not exceed a few ion plasma periods, so the ions are immobile and form a positive neutralizing background. In one spatial dimension and in the limit of weakly relativistic electron motion, Maxwell's equations and hydrodynamic equations of electron fluid give the coupled equations for the longitudinal and transverse momentum of electrons [29]

$$\left(\frac{\partial^2}{\partial t^2}+\omega_p^2\right)q_z = \frac{\omega_p^2}{2}q_z q^2 - \frac{c}{2}\frac{\partial^2 q^2}{\partial z \partial t} - cq_z\left(1-\frac{q^2}{2}\right)\frac{\partial}{\partial z}\left(\frac{\partial q_z}{\partial t}+\frac{c}{2}\frac{\partial q^2}{\partial z}\right), \quad (1a)$$

$$\left(\frac{\partial^2}{\partial t^2}-c^2\frac{\partial^2}{\partial z^2}+\omega_p^2\right)\mathbf{a}=\frac{\omega_p^2}{2}q^2\mathbf{a}-c\mathbf{a}\left(1-\frac{q^2}{2}\right)\frac{\partial}{\partial z}\times\left(\frac{\partial q_z}{\partial t}+\frac{c}{2}\frac{\partial q^2}{\partial z}\right). \quad (1b)$$

Here, $\mathbf{a}\equiv\mathbf{p}_{e\perp}/(m_ec)$ and $q_z\equiv p_{e_z}/(m_ec)$ are the normalized transverse and longitudinal components of the electron momentum, and $q^2\equiv q_z^2+\mathbf{a}_\perp^2<1$. We take $\mathbf{a}\equiv\mathrm{Re}(\mathbf{e}_0a)$, where $\mathbf{e}_0=(\mathbf{e}_x+i\mathbf{e}_y)/\sqrt{2}$ is a unit vector of circular polarization; hence, $q^2=q_z^2+|a|^2/2$. In the 1D approximation, conservation of the transverse canonical momentum expresses the normalized momentum through the laser vector potential, $\mathbf{A}_\perp=(m_ec^2/e)\mathbf{a}$. The normalized electron density perturbation

$$\frac{n_e-n_0}{n_0}\equiv\frac{\delta n}{n_0}\approx\frac{c}{\omega_p^2}\frac{\partial}{\partial z}\left[\frac{\partial q_z}{\partial t}+\frac{c}{2}\frac{\partial q^2}{\partial z}\right], \quad (2)$$

obeys the equation

$$\left(\frac{\partial^2}{\partial t^2}+\omega_p^2\right)\frac{\delta n}{n_0}-\frac{c}{2}\frac{\partial^2 q_z q^2}{\partial z\partial t}-\frac{c^2}{2}\frac{\partial^2 q_z^2}{\partial z^2}+c\frac{\partial^2}{\partial z\partial t}q_z\left(1-\frac{q^2}{2}\right)\frac{\delta n}{n_0}=\frac{c^2}{4}\frac{\partial^2|a|^2}{\partial z^2} \quad (3)$$

obtained through differentiating Eq. (1a) with respect to z and t. At the plasma entrance $z=0$, the amplitude of a planar two-frequency laser beam is given by

$$a(0,t)=e^{-i\omega_0 t}[a_0(0,t)+a_1(0,t)e^{-i\Omega t}], \quad (4)$$

where $\Omega\approx\omega_p\ll\omega_0$. The ponderomotive beat wave [the right-hand side (RHS) of Eq. (3)] produces an electron density grating comoving with the laser beams. The moving index grating produces the cascade of laser sidebands

$$a(z,t)=e^{-i\omega_0 t+ik_0 z}\sum_{l=-\infty}^{+\infty}a_l(z,t)e^{-il\Omega t+ilk_\Omega z}, \quad (5)$$

where $k_\Omega=\Omega/v_g$, and $v_g=k_0c^2/\omega_0$ is the group velocity associated with the laser fundamental frequency. v_g is found from $d\equiv n_0/n_c=1-(v_g/c)^2$, where $n_c=m_e\omega_0^2/(4\pi e^2)$ is a critical plasma density. The amplitudes a_n vary slowly in time and space on the scales Ω^{-1} and k_Ω^{-1}.

To describe the nonlinear evolution of the cascade (5), we take into account Eq. (2) and rewrite Eq. (1b) as

$$\left(\frac{\partial^2}{\partial t^2}-c^2\frac{\partial^2}{\partial z^2}\right)a+\omega_p^2a\left(1-\frac{q^2}{2}\right)\left(1+\frac{\delta n}{n_0}\right)=0. \quad (6)$$

We retain in Eq. (6) the terms of order not higher than a^3. Having in mind that $q_z\approx\delta n/n_0$, and that the relativistic saturation of the beat wave-driven EPW [8] occurs at $q_z\sim a^{2/3}$, we keep in Eq. (6) the nonlinear terms of order aq_z, a^3, aq_z^2, aq_z^3 and finally arrive at

$$\left(\frac{\partial^2}{\partial t^2}-c^2\frac{\partial^2}{\partial z^2}+\omega_p^2\right)a\approx\omega_p^2(R^a+R^q-C). \quad (7)$$

The terms

$$R^a=a|a/2|^2, \quad (8a)$$

$$R^q\approx(a/2)(\delta n/n_0)^2(1+\delta n/n_0) \quad (8b)$$

originating from the relativistic mass correction of an electron oscillating in the transverse (R^a) and longitudinal (R^q) fields describe the relativistic self-phase modulation of laser. The leading nonlinear current term

$$C=a(\delta n/n_0) \quad (9)$$

is responsible for the EMC and stimulated forward Raman cascade [30]. Our earlier work [16] assumed the nonresonant EPW excitation ($\delta n/n_0\sim a^2$), so the term (8b) was neglected. By including this term we include the regime with relativistic saturation of the resonantly driven EPW ($\delta n/n_0\sim a^{2/3}\gg a^2$).

We substitute the expansion (5) into Eq. (7), replace the variables (z,t) by (z,ξ) (where $\xi/v_g=t-z/v_g$ is a retarded time, and z is the propagation distance through plasma), and collect the equal frequency terms. The resulting set of coupled envelope equations

$$\left[2i\frac{\omega_l}{v_g}\frac{\partial}{\partial z}-\frac{d}{v_g^2}(\omega_l-\omega_0)^2\right]a_l\approx k_p^2(C_l-R_l^a-R_l^q), \quad (10)$$

where $k_p=\omega_p/c$, accounts for the propagation of sidebands through plasma [the first term in the left-hand side (LHS)], the GVD of the sidebands (the second term in the LHS), and the sideband coupling through the nonlinearities (the RHS). To evaluate the RHS of Eq. (10) we have to specify the nonlinear plasma response. The ponderomotive force [the RHS of Eq. (3)] approximated as $-(c/2)^2\Sigma_l(lk_\Omega)^2\rho_l(z,\xi)e^{ilk_\Omega\xi}$ drives the nonlinear density perturbation

$$\delta n(z,\xi)=\frac{1}{2}\sum_l\delta n_l(z,\xi)e^{ilk_\Omega\xi}, \quad (11)$$

where $\delta n_{-l}=\delta n_l^*$, $|\delta n_l|\ll n_0$, and $|\partial\delta n_l/\partial\xi|\ll k_\Omega|\delta n_l|$. The intensity momenta in Eq. (11) are

$$\rho_l=\sum_n a_n a_{n+l}^*, \quad (12)$$

and $|\partial\rho_l/\partial z|\ll k_\Omega|\rho_l|$. We assume that each density harmonic is driven by the corresponding harmonic of the ponderomotive force. The terms with $l=\pm1$ in Eq. (11) are the closest in frequency to the natural modes of plasma oscillations. They produce the dominant contribution to the cascade dynamics. Keeping in Eq. (3) the terms of order not higher than a^4, and having in mind the scaling $|\delta n/n_0|\sim a^{2/3}$ relevant to the case of relativistic saturation of the resonantly driven EPW [8], we find that the amplitude $N_e\equiv\delta n_{-1}(z,\xi)/n_c$ obeys the nonlinear equation

$$\left(\frac{i}{k_\Omega}\frac{\partial}{\partial\xi}+\frac{\delta\omega}{\Omega}\right)N_e+R=\frac{d}{4}\rho_{-1}. \quad (13)$$

Here, $\delta\omega=(\Omega^2-\omega_p^2)/(2\Omega)$ is the beat wave detuning from resonance, and R is proportional to the nonlinear frequency shift due to the relativistic mass increase of an electron oscillating in the longitudinal and transverse electric fields

$$R = \frac{3}{16} N_e \left| \frac{N_e}{d} \right|^2 + \frac{1}{8} (\rho_0 N_e + \rho_{-2} N_e^*). \quad (14)$$

The initial condition for Eq. (13) is $N_e(z,-\infty) \equiv 0$ (quiescent plasma ahead of the pulse). Amplitudes of the nonresonantly driven density harmonics ($l \neq \pm 1$) are found from the linearized Eq. (3)

$$\frac{\delta n_l(z,\xi)}{n_0} \approx \frac{1}{2} \frac{(\omega_l - \omega_0)^2}{(\omega_l - \omega_0)^2 - \omega_p^2} \rho_l(\xi, z). \quad (15)$$

Using Eqs. (15), we evaluate the nonlinear terms in the cascade equations (10). We extract from the terms C the contribution from the EPW harmonics of orders $l \neq \pm 1$ and include it into the terms R^a. Therefore, only the contribution from the near-resonant EPW harmonic N_e determines the form of the "cascade" nonlinearity C_l. And, only near-resonant EPW harmonic is taken into account for evaluating the terms R_l^q. The result is

$$C_l = \frac{N_e a_{l-1} + N_e^* a_{l+1}}{2d}, \quad (16a)$$

$$R_l^a \approx \frac{1}{4} \sum_n a_{n+l} \rho_n - \frac{1}{4} \sum_n{}' a_{n+l} \rho_n \frac{(\omega_n - \omega_0)^2}{(\omega_n - \omega_0)^2 - \omega_p^2}, \quad (16b)$$

$$R_l^q \approx \frac{1}{4} \left[\left| \frac{N_e}{d} \right|^2 \left(a_l + \frac{3}{4} \frac{N_e}{d} a_{l-1} + \frac{3}{4} \frac{N_e^*}{d} a_{l+1} \right) + \frac{1}{2} \left(\frac{N_e}{d} \right)^2 \left(a_{l-2} + \frac{1}{2} \frac{N_e}{d} a_{l-3} \right) + \frac{1}{2} \left(\frac{N_e^*}{d} \right)^2 \left(a_{l+2} + \frac{1}{2} \frac{N_e^*}{d} a_{l+3} \right) \right]. \quad (16c)$$

The second term in the RHS of Eq. (16b) comes from the nonresonant EPW harmonics (15), prime means that the terms with $n = \pm 1$ are not included in the sum. Physical meaning of the nonlinearities (16) is as follows.

(1) The terms C_l couple the neighboring laser sidebands through the *near-resonantly-driven* harmonic of the EPW. These terms describe the electromagnetic cascading and the stimulated forward Raman cascade.

(2) The terms R_l^a describe the nonlinear frequency shifts produced by the relativistic mass increase of an electron oscillating in the transverse fields and by the *nonresonantly-driven* harmonics of EPW.

(3) The terms R_l^q describe the nonlinear frequency shifts produced by the relativistic mass increase of an electron oscillating in the longitudinal electric field of the *nearresonantly-driven* harmonic of the EPW. Only when the EPW is driven resonantly and reaches the relativistic saturation the term R_l^q can dominate R_l^a. In all the simulations that will follow in this paper R_l^q's are negligibly small.

Assuming $v_g \approx c$, we rewrite the set (10) as

$$\left[\frac{2i}{k_0} \frac{\partial}{\partial z} - d \left(\frac{\omega_l - \omega_0}{\omega_0} \right)^2 \frac{\omega_0}{\omega_l} \right] a_l \approx d \frac{C_l - R_l^a - R_l^q}{\omega_l / \omega_0}. \quad (17)$$

The boundary condition for Eqs. (17) is given by Eq. (4). The weakly relativistic theory based on Eqs. (13) and (17) describes the nonlinear evolution of the plasma beat wave in one spatial dimension and in time. The nonlinear processes of the EPW excitation and bistability, the laser phase-self-modulation due to the relativistic frequency shifts, the electromagnetic cascading, and the FSRS are self-consistently included. The model also assumes the nonzero group velocity dispersion of radiation.

By the judicious choice of parameters the terms C_l can be made dominating in the RHS of Eq. (17), and laser spectral broadening will occur exclusively due to the EMC. Despite the large laser bandwidth achieved in certain regimes of EMC, the effect of GVD can be negligible (see the discussion at the bottom of Sec. II B). The laser amplitude can be then modified in a separate, denser, plasma with the high GVD (the compressor). In this two-stage scenario, nonlinearities of the modulator affect primarily the laser phase, while in the compressor the GVD modulates the amplitude. Compression of the laser beat notes in plasma can result in the laser intensity so high as to give $|a|^2 \sim 1$.

In the compressor, the laser sidebands remain coupled through the nonlinear frequency shifts, and the frequency bandwidth keeps growing. The relativistic nonlinearities of plasma can thus compete with the linear compression process. We choose the compressor density so as to entirely exclude the possibility of resonant plasma response: $\omega_{p(C)}$ is never close to an integer multiple of Ω. Provided $|l\rho_l| \ll 1$, the amplitude of density perturbation at the lth beat wave harmonic is described by Eq. (15) with n_0 and ω_p replaced by $n_{0(C)}$ and $\omega_{p(C)}$. As the electron density perturbations in the compressor are nonresonant and thus small, we neglect the terms R_l^q. Moreover, the terms C_l are absorbed by $R_l^a \equiv R_l^{a(C)}$ [that is, summation in the second term of Eq. (16b) is extended to $n = \pm 1$, and C_l's do not show up in the compressor equations]. We redefine the retarded time as $\zeta / v_{g(C)} = t - z / v_{g(C)}$ (where $v_{g(C)}$ is the group velocity of the laser fundamental component in the compressor plasma of density $n_{0(C)} \gg n_0$) and find that the compression process can be described in terms of the coupled nonlinear equations similar to Eqs. (17)

$$\left[\frac{2i}{k_0} \frac{\partial}{\partial z} - d_C \left(\frac{\omega_l - \omega_0}{\omega_0} \right)^2 \frac{\omega_0}{\omega_l} \right] a_l \approx - d_C \frac{\omega_0}{\omega_l} R_l^{a(C)}. \quad (18)$$

Here, $d_C = n_{0(C)} / n_c \ll 1$ is the normalized compressor density. The boundary conditions are given by the solution of Eqs. (17) at the modulator exit, $a_n(z = z_{\mathcal{M}}, \xi)$.

B. Basic scalings for laser frequency modulation and compression

In the ideal two-stage compressor sketched in Fig. 1, the processes of EMC and compression are separated. The EMC develops in the modulator plasma with zero GVD, while in the dense compressor plasma with all the nonlinearities ne-

glected the GVD compresses the radiation beat notes. It is instructive to derive the basic scalings for each process because these approximate scalings will help to select the optimal parameters of fully nonlinear simulations.

When both R_l^a and R_l^q are taken to be zero, and the GVD is neglected ($d=0$) in Eq. (17), scaling laws for the EMC are particularly simple. Assuming $\omega_l \approx \omega_0$, we derive from Eqs. (17) a set of conservation laws: $\partial \rho_l / \partial z = 0$. Hence, $\rho_l \equiv 0$ for $l \neq 0, \quad -1, \quad \rho_0(z,\xi) \equiv |a_0(0,\xi)|^2 + |a_1(0,\xi)|^2, \quad \rho_{-1}(z,\xi) \equiv a_1(0,\xi) a_0^*(0,\xi)$, and, in the comoving frame, N_e is independent of z despite the evolution of the laser phase. Thus simplified Eqs. (17) have the analytic solution [22]

$$a_l(z,\xi) = \sum_{\sigma=0,1} a_\sigma(0,\xi) e^{i(l-\sigma)(\psi+\pi)} J_{l-\sigma}(2W), \tag{19}$$

satisfying the initial condition (4) [here, $J_n(x)$ are the Bessel functions, and $\psi(z,\xi)$ and $W(z,\xi)$ are the phase and absolute value of the generating function $w(z,\xi) \equiv W e^{i\psi} = i(k_0 z/4) N_e(\xi)$]. Substituting Eqs. (19) into Eq. (5) yields the expression for a train of phase-modulated beat notes

$$a(z,\xi) = \sum_{\sigma=0,1} a_\sigma(0,\xi) \cos[k_\sigma \xi + \varphi(z,\xi)],$$

where $\varphi(z,\xi) = (k_0 z/2)|N_e(\xi)| \sin(\psi - k_\Omega \xi)$. The physical meaning of this result is that, without GVD, the laser undergoes frequency modulation only. The magnitude of the plasma wave depends only on the laser amplitude which remains unchanged. This is valid for any pair of $a_0(0,\xi)$, $a_1(0,\xi)$ and the corresponding $N_e(\xi)$.

The phase modulation is periodic in time with the beat period τ_b when $N_e(\xi)$ is almost constant (this is the case for $|\partial \rho_{-1} / \partial \xi| \ll |\delta\omega \rho_{-1}/c|$). To avoid the oscillations of N_e with time due to the relativistic dephasing [3,8,10], we take $|\delta\omega| \gtrsim 3(\omega_p/4)\sqrt[3]{3}|\rho_{-1}|^2/2$. Then, the term proportional to $\delta\omega$ dominates in the LHS of Eq. (13), which yields $N_e(\xi) \approx d[\rho_{-1}(\xi)/4](\Omega/\delta\omega)$; then, for real $\rho_{-1}(\xi)$,

$$a = \sum_{\sigma=0,1} a_\sigma(0,\xi) \cos[k_\sigma \xi + (k_0 z/2) N_e(\xi) \cos(k_\Omega \xi)]. \tag{20}$$

From Eq. (19), a modulator plasma slab of thickness

$$z_{\mathcal{M}} \approx 2\mathcal{M}/(N_e k_0) \tag{21}$$

produces $\mathcal{M}$ sidebands on either side of the fundamental, and a frequency bandwidth $\Delta\omega \sim 2\sqrt{d}\mathcal{M}\omega_0$. Conversely, $\mathcal{M} \sim r_e z_{\mathcal{M}} \lambda_0 |n_e - n_0|$, where $\lambda_0 = 2\pi c/\omega_0$ is the fundamental laser wavelength, and $r_e = e^2/(m_e c^2)$ is the classical electron radius.

As follows from Eq. (20), only for $\delta\omega < 0$ the laser wavelength shrinks with time near the amplitude maximum of each beat note (positive chirp). The GVD of plasma tends to compress thus chirped beat notes: the shorter (blueshifted) wavelengths catch up with the longer (redshifted) wavelengths, eventually building up the field amplitude near the beat note center. Thus, a sequence of sharp spikes is produced. If we consider an unperturbed compressor plasma of given density, neglect the relativistic effects by setting

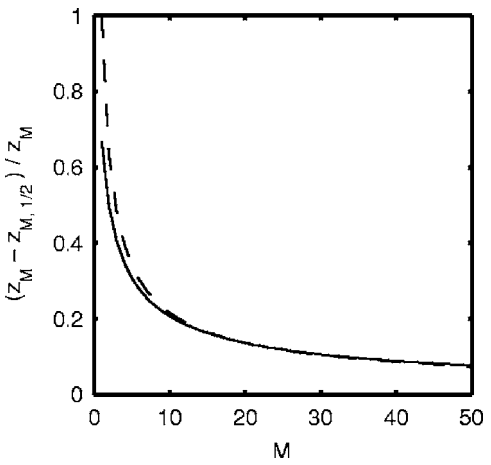

FIG. 2. Normalized distance between the points of the first maximum and half maximum of $J_M(z)$ (solid line) and the scaling function $M^{-2/3}$ (dashed line).

$R_l^{a(C)} \approx 0$ in Eq. (18), and fix laser frequency and the number $2\mathcal{M}$ of satellites, we find that the peak compression occurs at a distance

$$z_C \approx \frac{\pi/3}{k_0 \mathcal{M}} \left(\frac{\omega_0}{\omega_{p(C)}}\right)^2 \left(\frac{\omega_0}{\Omega}\right)^2. \tag{22}$$

This estimate assumes that the outer sidebands were initially separated in time by roughly $\tau_b/2$ within one beat note. To catch up with the red sidebands at the beat note center, the blue sidebands need the propagation time $z_C/c \approx (c/\Delta v_g)(\tau_b/2)$, where the group velocity mismatch is $\Delta v_g \approx 2\mathcal{M}\Omega(\partial v_g/\partial\omega)_{\omega_0} \approx (3\mathcal{M}\Omega/k_0)(\omega_{p(C)}/\omega_0)^2$.

The nonzero GVD of radiation in the modulator plasma must be properly accounted for. The cascade components can be redistributed in time and space thus reducing coherence of the EPW excitation and affecting the frequency chirp. Naively, the GVD can become significant if the modulator length $z_{\mathcal{M}}$ is close to the compression length estimated from Eq. (22) with $\omega_{p(C)} \equiv \omega_p$. However, the higher-order Stokes-anti-Stokes sidebands are generated later in plasma and have less time to catch up with the fundamental. Recalling that $|a_{\mathcal{M}}| \propto |J_{\mathcal{M}}(z)|$ in the modulator, we define the half-growth length $z_{\mathcal{M},1/2}$ at which $|a_{\mathcal{M}}|$ reaches a half of its maximum value, $|J_{\mathcal{M}}(z_{\mathcal{M},1/2})| = |J_{\mathcal{M}}(z_{\mathcal{M}})|/2$. Thereby, compression effectively takes place over the shorter distance $\Delta z \approx z_{\mathcal{M}} - z_{\mathcal{M},1/2} < z_{\mathcal{M}}$. The analytic formula $\Delta z \approx \mathcal{M}^{-2/3} z_{\mathcal{M}}$ accurately fits Δz for $\mathcal{M} \gtrsim 5$ (see Fig. 2). Therefore, $\Delta z \ll z_{\mathcal{M}}$ for $\mathcal{M} \gg 1$. Hence, for

$$z_{\mathcal{M}} \ll \mathcal{M}^{2/3} z_C \approx (\lambda_0/6)\mathcal{M}^{-1/3} d^{-2}, \tag{23}$$

the GVD effect is negligible because the distance Δz actually available for the compression in the modulator is less than z_C. Otherwise, if $z_{\mathcal{M}} \gtrsim \mathcal{M}^{2/3} z_C$, the GVD in the modulator becomes important.

Another manifestation of the GVD in the modulator is the SFRS seeded due to the finite duration of the beat wave pulse. The stimulated forward Raman cascading [30] can interfere with the process of phase modulation and contami-

nate the laser frequency chirp. Reduction in the compression efficiency can follow. The effect of SFRS is examined in Sec. III C.

III. NONLINEAR SIMULATIONS OF THE EMC

A. The two-stage cascade compressor

We model the EMC by numerically solving the set of coupled nonlinear equations (13) and (17) with the boundary condition

$$a_0(0,\xi) = a_1(0,\xi) = Ae^{-\xi^2/(c\tau_L)^2} \tag{24}$$

for the laser sidebands, and $N_e(z,\xi=-\infty)\equiv 0$ for the EPW. The beat note compression in the second stage is modeled by numerically solving the compressor equations (18). All the nonlinearities associated with the effects of relativistic mass correction and nonresonant electron density perturbations are retained in the modeling of both stages. In all the simulations below, the fundamental laser wavelength is fixed at $\lambda_0 = 0.8\ \mu$m.

The two-stage compression starts with the initial laser amplitude $A=0.2$, the modulator density $n_0=8.75\times10^{17}$ cm^{-3} (hence, $d=5\times10^{-4}$), and $\delta\omega=-0.1\omega_p$. The laser pulse duration is $\tau_L=4.5$ ps (about half the ion plasma period for a fully ionized helium). Having chosen the peak density perturbation $|N_e(z=0)|_{\max}\approx 0.5\times10^{-4}$ and expected final spectral width of the laser ($\mathcal{M}\approx 8$ sidebands on each side), we find the modulator length $z_8\approx 4.1$ cm. Importantly, the periodic phase modulation of the laser can be achieved only with the plasma wave driven quite far from resonance. Hence, the requirement of the plasma longitudinal homogeneity (which has always been a challenge for the original scheme of plasma beatwave accelerator [9]) is considerably relaxed. The present day technology is able to maintain highly (longitudinally) homogeneous plasmas over centimeter length scales. This can be done, for example, by confining the plasma in a differentially pumped cell [31] or in the ponderomotively created cm-long plasma channels [11,32].

The simulation results are shown in Fig. 3. From the plot (a) it is seen that the peak laser intensity at the compressor exit ($z=z_8+z_C$) is by a factor of 7.2 larger than at the modulator entrance ($z=0$). The increase in intensity results from the shown in plot (c) beat note compression from the initial duration of $\tau_{b(in)}\approx 120$ fs to $\tau_{b(out)}\approx 13$ fs (roughly 5 laser cycles). Compressor plasma has the density $n_{0(C)}=25n_0$ and length $\approx 0.0275z_8\approx 1.1$ mm (such a short dense plasma can be created by the ablation of a microcapillary [33]).

The inequality (23) is very well satisfied for the modulator parameters. Consequently, the beat note precompression seen in the plot (c) is quite insignificant. Plot (b) shows that $N_e(z,\xi)$ also reveals almost negligible variation with z in the modulator. Thereby, according to the plots (b) and (c), the EMC develops in accordance with the scenario outlined in Sec. II B.

Compression in the second stage clearly proceeds in the nonlinear regime. The laser amplitude becomes relativistic ($|a|\to 1$), and the nonlinear frequency shifts in Eqs. (18) couple the laser sidebands and further increase the laser bandwidth. Figure 3(d) shows that the resulting frequency spectrum is at least twice as broad if compared with that at the modulator exit. As a consequence, the linear formula (22) overestimates z_C by a factor of three since it ignores both precompression of the pulse in the modulator and additional bandwidth increase in the compressor. Also, quality of the compressed beat notes is not perfect: instead of a single sharp spike, one can observe a multispike structure in Fig. 3(c), the distance between the spikes being roughly $\tau_b/5$. One can relate this structure to the phase modulation occurring due to the electron density perturbation at fifth harmonic of the beat wave frequency, which is the closest to the natural mode of the compressor plasma oscillations. Due to this effect, one beat note is not gradually compressed into one spike but rather splits into five spikes, of which the one located near the original beat note maximum has the largest amplitude.

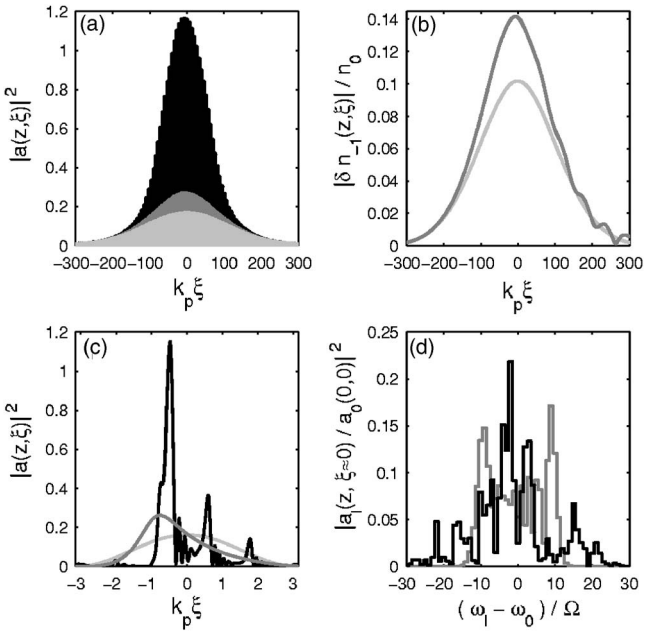

FIG. 3. The two-stage cascade compression. The physical quantities are shown at the entrance ($z=0$, light gray) and exit of the modulator ($z=z_8$, medium gray), and after the compressor ($z=z_8+z_C$, black). (a) The laser pulse intensity (the time window contains about 100 beat notes). (b) The normalized amplitude of the near-resonant EPW, $\delta n_{-1}/n_0=N_e/d$. (c) The beat note intensity near the laser pulse center; one beat period near $\xi=0$ is shown. (d) The laser spectra near $\xi=0$. The nonlinearities and GVD in both plasmas are included.

A number of issues are yet to be addressed before the theory of the two-stage compression is complete. The neglected effects of transverse evolution of the laser, such as relativistic self-focusing and cascade focusing [3], are dominant at high plasma density in the compressor and are potentially adverse. But, we find the 1D scenario of the two-stage compression conceptually simple and helps to understand the underlying phenomena. In the next section we consider the single-stage approach which assumes concurrent cascading and compression in the same low-density plasma.

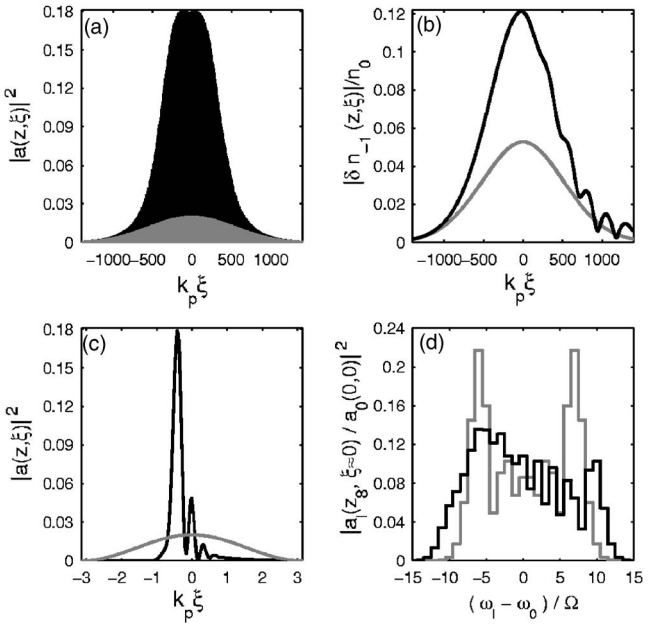

FIG. 4. The single-stage compressor with concurrent EMC and compression. In plots (a)–(c), the physical quantities are shown at the entrance ($z=0$, gray) and exit of the plasma ($z=z_8$, black). (a) The laser pulse intensity (the time window contains about 500 beat notes). (b) The normalized amplitude of the near-resonant EPW, $\delta n_{-1}/n_0=N_e/d$. (c) The beat note intensity near the laser pulse center, $\xi=0$. (d) The laser spectra near $\xi=0$ with (black) and without (gray) GVD and all nonlinear frequency shifts.

B. The single-stage cascade compressor

Increasing plasma density in the modulator increases the GVD. Therefore, we can explore the idea of compressing the beatnotes concurrently with generating the sidebands. In the following set of simulations the electron density is doubled, $n_0=1.75\times10^{18}$ cm^{-3}. Cascade compression is simulated in plasma of the same length, $z_8=4.1$ cm, and with the same initial density perturbation $|N_e(z=0)|_{\max}\approx0.5\times10^{-4}$ as in the previous section. The laser amplitude is $A\approx0.071$, and the beat wave detuning is $\delta\omega=-0.025\omega_p$. As we shall see in Sec. III C, the SFRS manifestation can be large in this regime. Appropriately low seed level can be achieved with the beat wave pulse envelope varying slowly on the time scale $\delta\omega^{-1}$. We choose the beat wave pulse $\tau_L=14.25$ ps long (which is about three ion plasma periods for a fully ionized helium), which corresponds to $|\delta\omega\tau_L|\approx27$. The given initial intensity on axis and laser duration would require the pulse energy of about 5 J in the focal spot of 30 μm radius.

The linear estimate of the effective compression length (22) shows that the inequality (23) almost breaks under the simulation parameters. Hence, a beat note compression is large at the plasma exit. Figure 4(a) shows that the resulting peak intensity is by an order of magnitude larger than at the plasma entrance. Initial duration of the laser beat note, as shown in Fig. 4(c), is reduced from $\tau_{b(in)}\approx85$ fs by roughly a factor of 10 (to roughly 3 laser cycles). The spectral features of the EMC are different from those obtained with the nonlinear frequency shifts and the GVD neglected [i.e., with $d=0$ in Eqs. (17)]. A red asymmetry of the cascade spectrum is seen in Fig. 4(d). Some spectral broadening versus the case of $d=0$ can be attributed to the self-phase modulation produced by the nonlinear frequency shifts. Figure 4(b) shows that the electron density perturbation is not an integral of motion. Its final amplitude is roughly twice the initial, and a small-amplitude wake is left behind the train of compressed spikes which can be recognized as a signature of SFRS. However, under parameters chosen, neither the self-phase modulation nor the SFRS are adverse for the cascade compression.

The transverse evolution of the cascade is an aspect of high importance of the realistic laser and plasma dynamics. For instance, electron density perturbations can significantly reduce the nonlinear focusing threshold of counterpropagating laser beams [4]. The copropagating cascade of electromagnetic beams also experiences enhanced focusing in both 2D (planar) and 3D (cylindrical) geometry if $\Omega<\omega_p$ (Refs. [2,3]). We shall give here a few necessary estimates (effects of transverse evolution will be given a detailed consideration in the forthcoming publications). When the beat wave is downshifted by $\delta\omega=-3(\omega_p/4)\sqrt[3]{3|\rho_{-1}|^2}/2$, the self-focusing threshold in the planar 2D geometry [2,3] is $a_0(k_px_0/10)^3\geqslant0.064$, where x_0 is a laser focal spot size ($a=a_0e^{-x^2/x_0^2}$). So, the subthreshold regime under the parameters of Figs. 3 and 4 requires the spot size $x_0<40$ μm. If we loosely translate x_0 into the radius of the laser focal spot in the cylindrical geometry, we find that the refraction-limited interaction length $2z_R=(2\pi/\lambda_0)x_0^2$ is less than 1.2 cm. However, the required $z_8\approx4.1$ cm can be achieved by means of the plasma channel guiding [32].

In the regime of cascade compression considered above, eliminating potentially adverse effects of laser self-phase modulation and SFRS required complying with some hard restrictions on the laser pulse amplitude, duration, and beat wave frequency detuning ($|a|^2\ll1$, and $|\delta\omega\tau_L|\gg1$). The next set of simulations shows that these conditions are desirable but not necessary for the manifestation of the effect. The cascade compression can be observed even for ultrashort (~100 fs) beat wave pulses propagating in a dense plasma ($n_0\sim10^{19}$ cm^{-3}) where neither GVD nor relativistic nonlinearities are small. We consider the evolution of a two-color ultrashort laser [28] whose energy is initially distributed between the fundamental (97%) and the Stokes (3%) components. The laser frequencies are $\omega_0=2.356\times10^{15}$ s^{-1} ($\lambda_0=0.8$ μm) and $\omega_1=2.159\times10^{15}$ s^{-1} ($\lambda_1=0.873$ μm). Assuming that $\omega_0-\omega_1=0.95\omega_p$, we derive the plasma density $n_0=1.35\times10^{19}$ cm^{-3}; hence, $d=7.725\times10^{-3}$. We choose $a_0\approx0.3$, and $a_1\approx0.048$. At $z=0$, the laser pulse is Gaussian (24) with a duration $\tau_L\approx90$ fs. In this case $|\delta\omega\tau_L|\approx0.9$, and the beat wave pulse amplitude is not slowly varying. Nevertheless, under these seemingly unfavorable conditions, the EMC develops very effectively and the intensity contrast of the amplitude-modulated laser pulse grows rapidly. The plasma length is chosen so as to produce five sidebands on either side; the plasma length is bounded from above by $z_5\approx2.5$ mm, while the compression length evaluated from formula (22) for $\mathcal{M}=5$ gives the lower bound, $z\approx0.45$ mm. The most spectacular features of the EMC shown in Fig. 5 are observed at $z\approx1.8$ mm. At the plasma border, $z=0$, the

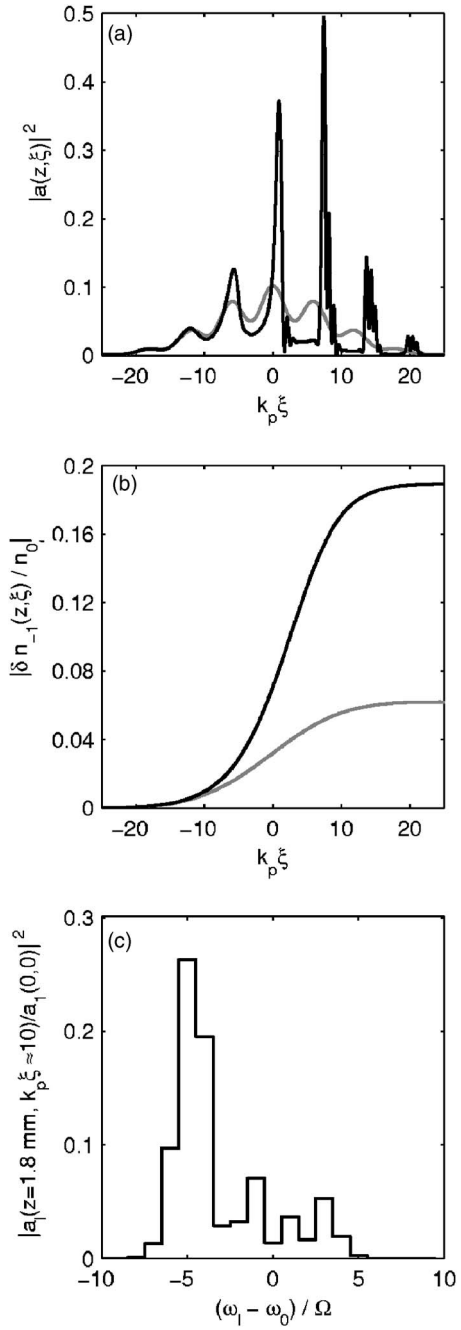

FIG. 5. The EMC of the two-color short-pulse (90 fs) laser [28] in a dense (1.35×10^{19} cm^{-3}) plasma. Physical quantities are shown at the plasma entrance ($z=0$, gray lines) and exit ($z=1.8$ mm, black lines).

intensity variation of the two-color laser is about 50%, while at $z\approx1.8$ mm very deep amplitude modulation develops with the intensity contrast ratio reaching a factor of 25. The mostly affected are the beat notes in the tail of the laser pulse; they are compressed to roughly a quarter of a plasma period. The laser nonlinear evolution boosts the amplitude of the plasma wake (which is increased by a factor of 3). The laser spectrum broadens and reveals a redshift by about $-\omega_0/2$. This is a clear indication of the forward stimulated Raman cascade [30] which, as appears in this simulation, does not prevent the beat note compression. Moreover, the laser frequency redshifts towards the pulse tail. The redshifted field components that form the compressed beat notes in the tail move slower than those in the pulse head. Thus, as seen in Fig. 5(a), the beat notes in the tail accumulate a considerable time delay (about a quarter of the beat period) with respect to the initial positions of their maxima. This time delay is in agreement with the frequency shift $-\omega_0/2$.

The simulations presented in this section demonstrate the robustness of the EMC in the conditions when the GVD is large, and the nonlinear processes of the relativistic self-phase modulation and the SFRS interfere the cascading process. Slow variation of the beat wave pulse envelope is therefore helpful but not necessary for the cascade compression.

C. Manifestation of SFRS in cascade compressor

Equations (17) admit the longitudinal transfer of electromagnetic energy in the comoving frame. Therefore, the laser amplitude modulation may result not only from the EMC with concurrent compression of beatnotes but also from the SFRS instability [19,20,30] (also referred to as the 1D resonant modulational instability [5]). The SFRS is different from the EMC. The latter is merely a phase modulation which may proceed in the absence of GVD.

The SFRS is a resonant process seeded by the electron density perturbations oscillating at the plasma frequency ω_p. The instability bandwidth is much narrower than ω_p even in the case of relativistically strong pump, $a_0\sim1$ (Ref. [20]). And, in the examples of Figs. 3 and 4, the SFRS bandwidth is much lower than the absolute value of the beat wave frequency detuning $\delta\omega$. However, an electron plasma response to the laser beat wave *always* contains a component oscillating at ω_p. This component is due to the finite duration of the beat wave pulse, and its amplitude is governed by the product $|\delta\omega\tau_L|$. These resonant density perturbations can be enhanced by the SFRS to a level comparable to that of a nonresonant plasma response, and can interfere the phase modulation process. Hence, the effect of the SFRS is adverse and should be avoided by the judicious choice of laser and plasma parameters.

The seed level for the SFRS can be reduced by taking $|\delta\omega\tau_L|\gg1$. For example, parameters used in Figs. 3 and 4 correspond to $|\delta\omega\tau_L|\sim30$ and reveal no SFRS manifestation: no considerable plasma wake is left behind the laser at $z=z_8$. Hence, the plasma response is almost entirely nonresonant in these simulations.

Under parameters of Fig. 3, reduction in the beat wave pulse duration by a factor of 2.5 ($|\delta\omega\tau_L|=10$) produces visible enhancement of the plasma wake that can be attributed to the SFRS manifestation (see Fig. 6). At the plasma border, the wake amplitude is $\delta n(z=0)\equiv\delta n_s\approx2.4\times10^{-3}n_0$. Taking δn_s as the SFRS seed amplitude, we can theoretically evaluate the amplification factor by using the formula (4.12) of Ref. [20], $\ln|\delta n(z)/\delta n_s|\approx(2/c)[z\int_{-\infty}^{+\infty}\Gamma_0^2(\tau)d\tau]^{1/2}$. This expression takes into account the laser temporal profile and is valid for $z\gg\xi\gg c\tau_L$; $\Gamma_0^2(\tau)=(1/8)(\omega_p^4/\omega_0^2)a_0^2(\tau)$ stands for the instantaneous growth rate. The theoretical estimate of the amplification factor is $\ln|\delta n(z_8)/\delta n_s|\approx3.36$. On the other hand,

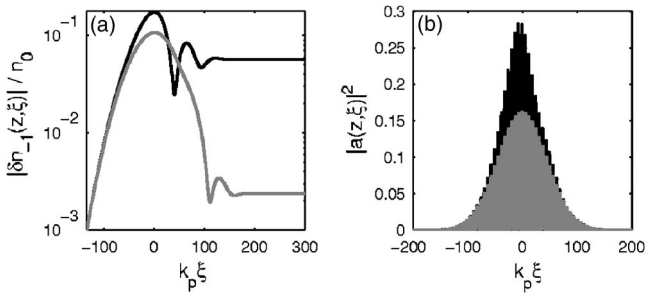

FIG. 6. Electron density perturbation (a) and the temporal profile of laser intensity (b) for the parameters the same as of Fig. 3 except the laser duration reduced by a factor of 2.5, $\omega_p\tau_L \approx 100$. Gray color corresponds to $z=0$, black—to $z=z_8$.

comparing the wake amplitudes at the entrance ($z=0$) and at the exit ($z=z_8$) of the plasma gives the amplification factor of $\ln|\delta n(z_8)/\delta n_s| \approx 3.2$, which is very close to the analytical estimate. We have found that the theory and simulation agree for $80 < \omega_p\tau_L < 300$. Therefore, throughout this range, plasma wakes are excited almost entirely by the SFRS. Remarkably, the peak laser intensity, as well as the shape of individual beat notes, is almost the same at $z=z_8$ for the parameters of Figs. 3 and 6. Hence, in the considered parameter range the effect of SFRS has a negligible effect on the laser evolution.

Oppositely to the just discussed case of rarefied plasma, reducing the laser duration by the same factor 2.5 under the parameters of Fig. 4 (i.e., the plasma twice as dense versus that of Figs. 3 and 6) causes significant enhancement of SFRS. Figure 7(a) shows the plasma wake amplification by a factor of $\ln|\delta n(z_8)/\delta n_s| \approx 6.05$. Theoretical estimate of the SFRS gain gives 4.2; this discrepancy can be partly explained by the laser amplitude growth due to the beat note compression. Figure 7(b) demonstrates the strong deformation of the beat wave intensity profile. The spectral content of the electromagnetic cascade varies considerably and can exhibit either overall red or blue shift at different ξ in the window $-100 < k_\Omega\xi < 100$.

In conclusion, to get rid of the SFRS, one should keep the SFRS seed low by keeping the product $|\delta\omega\tau_L|$ very large. As the simulations show, it should exceed 20; this may require the beat wave pulse of several picoseconds or even longer.

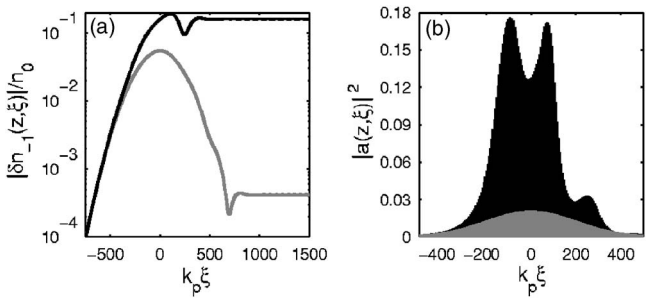

FIG. 7. Electron density perturbation (a) and the temporal profile of laser intensity (b) for the parameters the same as of Fig. 4 except the laser duration reduced to $\omega_p\tau_L \approx 440$, and $|\delta\omega\tau_L| = 10$. Gray color corresponds to $z=0$, black—to $z=z_8$.

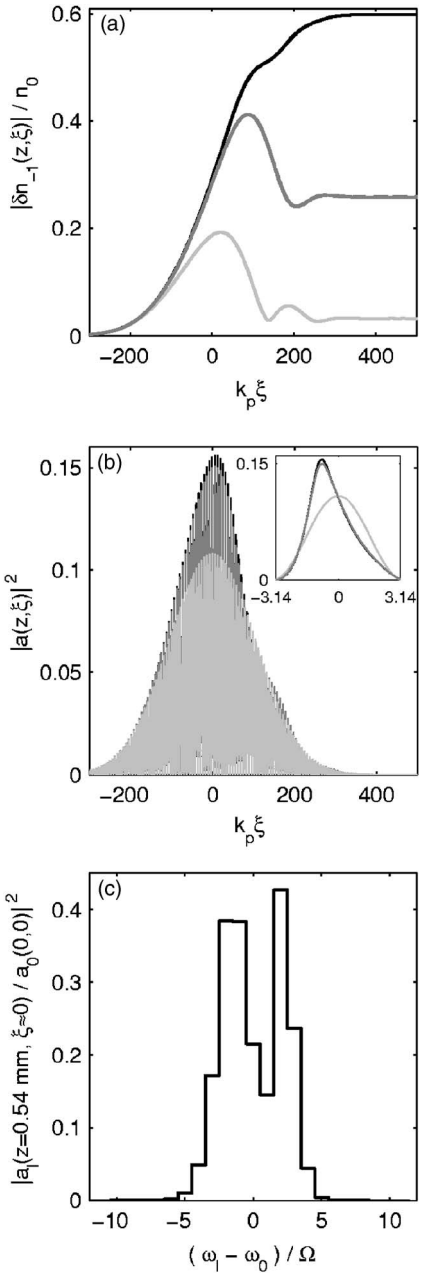

FIG. 8. Relativistic bistability of the EPW. Magnitude of the near-resonant electron density perturbation [plot (a)] and the laser intensity [plot (b)] are shown at $z=0$ (light gray), $z=0.52$ mm (medium gray), and $z=0.54$ mm (black). Inset in plot (b): one beat note selected near $\xi=0$. Plot (c): the laser spectrum at $z=0.54$ mm. The RB threshold is crossed at $z \approx 0.53$ mm. Crossing the threshold increases the EPW amplitude by a factor of 2.3.

D. Relativistic bistability of EPW

Cascade compression is a perfect tool for studying threshold phenomena. One of them, the relativistic bistability (RB) of the EPW driven by the long ($|\delta\omega\tau_L| \gg 1$) beat wave pulse with $\Omega < \omega_p$, is considered in this section. The RB results in the excitation of large-amplitude plasma wakes [14]. The intensity threshold should be met for the RB to occur. The threshold is multifaceted: it is determined by the beat wave

frequency detuning $\delta\omega$, the laser amplitude, shape, duration, contribution from the plasma wave harmonics, etc. Various aspects of the RB in the approximation of the prescribed (nonevolving) driver $\rho_{-1}(\xi)$ are addressed in Ref. [15]. Now, with the help of the cascade compression effect, we are showing for the first time that the RB can manifest in the dynamic simulations with the laser initially not optimized to meet the bistabilty threshold.

The laser amplitude modulation becomes important when the propagation over a considerable distance in plasma is concerned. Strong distortion of the beatwave temporal profile within a finite distance (few millimeters) in a dense ($n_0 \sim 10^{19}$ cm^{-3}) plasma does have adverse consequences for the amplitude- and phase-sensitive process of RB. On the other hand, we demonstrate below that the beat note compression helps to cross the RB threshold in the case of initially subthreshold laser amplitude. We start the simulation with the parameters of the numerical example from Ref. [14]: simulation starts at $z=0$ in a plasma with a density $n_0 = 10^{19}$ cm^{-3}, the beat wave pulse having a Gaussian temporal profile (24) with $\omega_p \tau_L \approx 212$ and $\delta\omega = -0.05\omega_p$, and the laser fundamental wavelength being $\lambda_0 = 0.8\ \mu$m (then, $d \approx 0.0057$). Solution of Eq. (13) with a given driver (equivalent to the calculations of plasma response at the entrance point $z=0$) gives the RB threshold $A^2 \approx 0.034$ (16% lower than in Ref. [14]). This threshold corresponds to the normalized peak intensity $|a|^2_{\max} \approx 0.136$. To demonstrate how this threshold is crossed in the course of laser evolution in plasma, we start the simulation with a sub-threshold value of the laser intensity, $A^2 \approx 0.027$. The simulation results are shown in Fig. 8.

As the laser travels through plasma, the cascade compression of the beat notes locally increases the intensity, and the RB threshold is crossed at a distance $z \approx 0.53$ mm. At this point, the magnitude of the electron density perturbation jumps abruptly by a factor of 2.3 [$\delta n_{-1}/n_0$ immediately before and after crossing the RB threshold is shown in Fig. 8(a)]. After that point, the resonant density perturbation grows steadily to roughly 80% of background density. At $z \approx 1.2$ mm the beat wave amplitude distortion becomes so strong as to destroy the coherence of the plasma response, and δn_{-1} drops sharply. Importantly, at the point where the RB threshold is met, the beat note profile is not very different from sinusoidal [see the inset in Fig. 8(b)], and the shape of the beat wave pulse is not much different from the initial Gaussian. The normalized intensity at which the RB occurs in the simulation is $|a|^2_{\max} \approx 0.145$. The amplitude of the beat wave pulse immediately before ($z=0.52$ mm) and after ($z=0.54$ mm) crossing the RB threshold is almost the same, as can be seen in the plot Fig. 8(b). As follows from Fig. 8(c), the beat note compression necessary for reaching the RB threshold is achieved at the laser bandwidth roughly equal to $\omega_0/3$.

Therefore, the proposed model of EMC in plasmas with nonzero GVD is able to demonstrate the effect of relativistic bistability in the dynamic simulations with initially subthreshold laser amplitude.

IV. CONCLUSION

In this paper, we have developed a nonlinear model that comprehensively describes the evolution of laser beat wave and electron density perturbations in time and in 1D in space in the weakly relativistic regime. Electromagnetic spectrum evolution and the effects of nonzero group velocity dispersion are accurately modeled. The model includes the nonlinear frequency shifts related to the relativistic corrections of electron mass and the harmonics of the electron density perturbations. It also takes into account the spatio-temporal evolution of the near-resonantly driven electron density perturbation. The theoretical model also describes a number of nonlinear effects important for the implementation of plasma beat wave accelerator. It is found that, for the beat wave downshifted in frequency from the plasma resonance, the electromagnetic cascading produced by the near-resonant electron density perturbations leads to the compression of the laser beat notes, which finally transforms the beat wave pulse into a train of sharp (few laser cycle) electromagnetic spikes separated by the beat period in time and space. A train of electromagnetic pulses useful for the particle acceleration applications [24–26] can be self-consistently created. We are also able to demonstrate how the electron plasma wave of large amplitude can be excited due to the effect of relativistic bi-stability even in the case of initially subthreshold beat wave pulse.

ACKNOWLEDGMENTS

The work is supported by the U.S. Department of Energy under Contracts No. DE-FG02-04ER54763 and DE-FG02-04ER41321, by the National Science Foundation Grant No. PHY-0114336 administered by the FOCUS Center at the University of Michigan, Ann Arbor.

[1] S. C. Wilks, J. M. Dawson, W. B. Mori, T. Katsouleas, and M. E. Jones, Phys. Rev. Lett. **62**, 2600 (1989); E. Esarey, A. Ting, and P. Sprangle, Phys. Rev. A **42**, 3526 (1990).

[2] P. Gibbon and A. R. Bell, Phys. Rev. Lett. **61**, 1599 (1988); **61**, 2509 (1988); **65**, 1962 (1990); E. Esarey and A. Ting, *ibid.* **65**, 1961 (1990).

[3] P. Gibbon, Phys. Fluids B **2**, 2196 (1990).

[4] G. Shvets and A. Pukhov, Phys. Rev. E **59**, 001033 (1999).

[5] N. E. Andreev, L. M. Gorbunov, V. I. Kirsanov, A. A. Pogosova, and A. S. Sakharov, Plasma Phys. Rep. **22**, 739 (1996).

[6] G. Shvets, N. J. Fisch, A. Pukhov, and J. Meyer-ter-Vehn, Phys. Rev. Lett. **81**, 4879 (1998); V. M. Malkin, G. Shvets, and N. J. Fisch, Phys. Rev. Lett. **82**, 4448 (1999).

[7] J. Faure, Y. Glinec, J. J. Santos, F. Ewald, J. P. Rousseau, S. Kiselev, A. Pukhov, T. Hosokai, and V. Malka, Phys. Rev. Lett. **95**, 205003 (2005).

[8] M. N. Rosenbluth and C. S. Liu, Phys. Rev. Lett. **29**, 701 (1972).

[9] T. Tajima and J. M. Dawson, Phys. Rev. Lett. **43**, 267 (1979).
[10] C. M. Tang, P. Sprangle, and R. N. Sudan, Phys. Fluids **28**, 1974 (1985).
[11] S. Ya. Tochitsky, R. Narang, C. V. Filip, P. Musumeci, C. E. Clayton, R. B. Yoder, K. A. Marsh, J. B. Rosenzweig, C. Pellegrini, and C. Joshi, Phys. Rev. Lett. **92**, 095004 (2004); Phys. Plasmas **11**, 2875 (2004); C. V. Filip, R. Narang, S. Ya. Tochitsky, C., E. Clayton, P. Musumeci, R. B. Yoder, K. A. Marsh, J. B. Rosenzweig, C. Pellegrini, and C. Joshi, Phys. Rev. E **69**, 026404 (2004).
[12] B. Walton, Z. Najmudin, M. S. Wei *et al.*, Opt. Lett. **27**, 2203 (2002); Phys. Plasmas **13**, 013103 (2006).
[13] R. R. Lindberg, A. E. Charman, J. S. Wurtele, and L. Friedland, Phys. Rev. Lett. **93**, 055001 (2004).
[14] G. Shvets, Phys. Rev. Lett. **93**, 195004 (2004).
[15] S. Kalmykov, O. Polomarov, D. Korobkin, J. Otwinowski, J. Power, and G. Shvets, Philos. Trans. R. Soc. London, Ser. A **364**, 725 (2006).
[16] S. Kalmykov and G. Shvets, Phys. Rev. Lett. **94**, 235001 (2005).
[17] W. B. Mori, IEEE J. Quantum Electron. **QE-33**, 1879 (1997).
[18] C. Max, J. Arons, and B. Langdon, Phys. Rev. Lett. **33**, 209 (1974); I. Watts, M. Zepf, E. L. Clark, M. Tatarakis, K. Krushelnick, A. E. Dangor, R. Allott, R. J. Clarke, D. Neely, and P. A. Norreys, Phys. Rev. E **66**, 036409 (2002).
[19] W. B. Mori, C. D. Decker, D. E. Hinkel, and T. Katsouleas, Phys. Rev. Lett. **72**, 1482 (1994).
[20] A. S. Sakharov and V. I. Kirsanov, Phys. Rev. E **49**, 3274 (1994).
[21] B. I. Cohen, A. N. Kaufman, and K. M. Watson, Phys. Rev. Lett. **29**, 581 (1972).
[22] S. J. Karttunen and R. R. E. Salomaa, Phys. Rev. Lett. **56**, 604 (1986); Phys. Scr. **33**, 370 (1986).
[23] S. E. Harris and A. V. Sokolov, Phys. Rev. Lett. **81**, 2894 (1998); Fam Le Kien, K. Hakuta, and A. V. Sokolov, Phys. Rev. A **66**, 023813 (2002).
[24] D. Umstadter, E. Esarey, and J. Kim, Phys. Rev. Lett. **72**, 1224 (1994).
[25] S. Dalla and M. Lontano, Phys. Rev. E **49**, R1819 (1994).
[26] G. Bonnaud, D. Teychenné, and J.-L. Bobin, Phys. Rev. E **50**, R36 (1994).
[27] P. Mora, D. Pesme, A. Héron, G. Laval, and N. Silvestre, Phys. Rev. Lett. **61**, 1611 (1988).
[28] F. Grigsby, D. Peng, and M. Downer, Stimulated Raman Scattering and Compression of Chirped TW Laser Pulses for Two-Color High Intensity Experiments, presented at the CLEO/QELS and *PhAST* 2005, Baltimore, MD (unpublished).
[29] L. M. Gorbunov, P. Mora, and T. M. Antonsen, Jr., Phys. Plasmas **4**, 4358 (1997).
[30] Baiweh Li, S. Ishiguro, M. M. Škorić, Min Song, and T. Sato, Phys. Plasmas **12**, 103103 (2005).
[31] R. Zgadzaj, E. W. Gaul, N. H. Matlis, G. Shvets, and M. C. Downer, J. Opt. Soc. Am. B **21**, 1559 (2004).
[32] E. Esarey, P. Sprangle, J. Krall, and A. Ting, IEEE Trans. Plasma Sci. **PS-24**, 252 (1996).
[33] A. Yu. Goltsov, D. V. Korobkin, Y. Ping, and S. Suckewer, J. Opt. Soc. Am. B **17**, 868 (2000).